Modeling active cellular transport as a directed search process with stochastic resetting and delays

Paul C. Bressloff

Department of Mathematics, University of Utah, Salt Lake City, Utah 84112, USA

E-mail: bressloff@math.utah.edu

Abstract. We show how certain active transport processes in living cells can be modeled in terms of a directed search process with stochastic resetting and delays. Two particular examples are the motor-driven intracellular transport of vesicles to synaptic targets in the axons and dendrites of neurons, and the cytoneme-based transport of morphogen to target cells during embryonic development. In both cases, the restart of the search process following reset has a finite duration with two components: a finite return time and a refractory period. We use a probabilistic renewal method to explicitly calculate the splitting probabilities and conditional mean first passage times (MFPTs) for capture by a finite array of contiguous targets. We consider two different search scenarios: bounded search on the interval $[0, L]$, where L is the length of the array, with a refractory boundary at $x = 0$ and a reflecting boundary at $x = L$ (model A), and partially bounded search on the half-line (model B). In the latter case there is a non-zero probability of failure to find a target in the absence of resetting. We show that both models have the same splitting probabilities, and that increasing the resetting rate r increases (reduces) the splitting probability for proximal (distal) targets. On the other hand the MFPTs for model A are monotonically increasing functions of r, whereas the MFPTs of model B are non-monotonic with a minimum at an optimal resetting rate. We also formulate multiple rounds of search-and-capture events as a $G/M/\infty$ queue and use this to calculate the steady-state accumulation of resources in the targets.

1. Introduction

One of the limitations of a purely diffusive process as a mechanism for the stochastic search for some hidden target in an unbounded domain is that the mean first passage time (MFPT) for target detection is infinite. However, the introduction of stochastic resetting, whereby the position of the searcher is reset to a fixed location over a random sequence of times, leads to a finite MFPT that has a unique minimum as a function of the resetting rate [12, 13, 14]. These observations have motivated numerous studies of more general stochastic processes with resetting, including non-diffusive processes such as Levy flights [20] and active run and tumble particles [15], resetting in bounded domains [25], resetting followed by a refractory period [16, 23] (which arises in certain Michaelis-Menten reaction schemes [28, 29, 30]), and resetting with finite return times [26, 22, 27, 3]. (For further extensions and applications see the review [17] and references therein.)

Recently, we considered another example of a stochastic process with an infinite MFPT being rendered finite by resetting, namely, a directed intermittent search process [7]. In particular, we analyzed a biased velocity jump process in which a particle switches between a stationary state and right-moving ballistic state according to a two-state Markov process. The particle can be captured by a target (or one of a set of targets) at a fixed rate whenever it is in the stationary state and within range of the target. In addition, the particle can reset its position to the origin at some rate r. In the absence of resetting there is a non-zero probability that the particle moves beyond the target(s) without being captured, resulting in an infinite MFPT. Directed intermittent search with multiple targets also has certain analogies with the example of mortal walkers, where there are two possible outcomes of the search process, namely, target detection or death [34, 10, 2].

As highlighted in [7], there are various examples of directed search processes in cell biology [4], including motor-driven intracellular transport of vesicles to synaptic targets in the axons and dendrites of neurons [31, 11, 21], and the transport of morphogen at the tips of growing actin-rich filaments (cytonemes) to target cells during embryonic development in vertebrates [32, 19, 33]. In the first example the particle (searcher) represents a molecular motor complex moving along a polymerized filament such as a microtubule within the axon or dendrite of a neuron, while resetting corresponds to the removal and return of the complex to the cell body, see Fig. 1. On the other hand, in the second example the particle represents the tip of a growing cytoneme, while resetting takes into account the fact that a cytoneme can suddenly switch to a shrinkage phase and rapidly retract back to the source cell, see Fig. 2. In our previous study [7], we assumed for simplicity that resetting was instantaneous and that the particle immediately reentered the search phase. However, this neglects the fact that the restart of the search process following reset has a finite duration with two components: a finite return time and a refractory period. In terms of the two given examples, the return time would depend on the speed of retrograde motor transport or the rate of cytoneme retraction, while the refractory period would depend on the time to reload a motor complex with vesicles at the cell body or the time for a new cytoneme to nucleate from the source cell.

Another important characteristic feature of the cell transport processes shown in Figs. 1 and 2 is that the arrival of a particle at a target results in the delivery of some resource. In the case of a motor-cargo complex, the resource could be synaptic proteins bound to a vesicle [31, 11, 21]. On the other hand, cytonemes in vertebrates

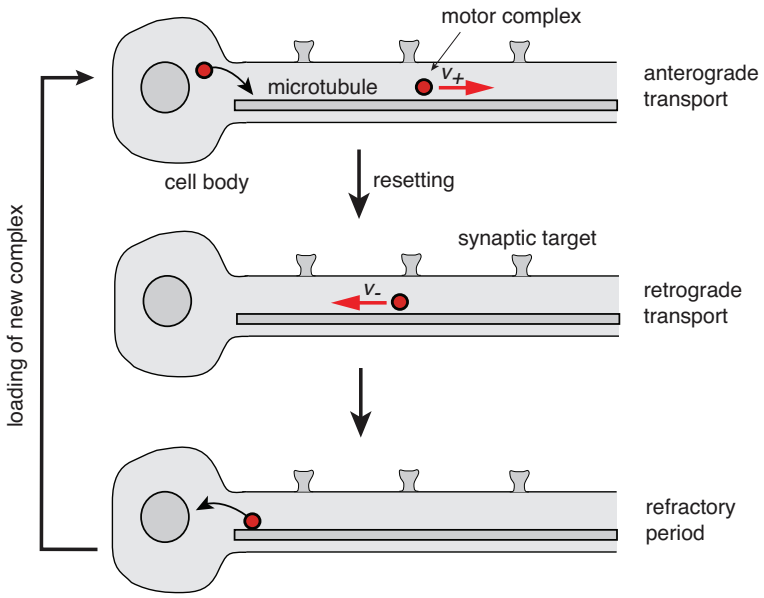

Figure 1: Search-and-capture model of motor driven intracellular transport. A motor-cargo complex moves ballistically with speed v_+ away from the cell body and searches for a synaptic target to deliver its cargo. Prior to finding a target, the complex may randomly switch to a retrograde state (resetting) and return to the cell body at a speed v_-. After a refractory period, a new motor complex is inserted onto the microtubule.

carry morphogen at their tips, which is released to the target cell after being captured [32, 19, 33]. Following delivery of its cargo, the particle escapes and may return to its initial (reset) position where it is reloaded with supplies in order to initiate a new search process. This would then lead to a sequence of search-and-capture events, whereby resources accumulate in the targets. Assuming that the build up of resources within each target is counterbalanced by degradation, there will exist a steady-state number of packets in the long-time limit. One way to calculate the statistics of resource accumulation is to formulate multiple search-and-capture events as a $G/M/\infty$ queue. This was originally explored within the context of a cytoneme-based transport model without resetting, where queueing theory was used to analyze the accumulation of morphogen in a one-dimensional (1D) array of target cells. More recently, we have applied queueing theory to a general class of search processes with stochastic resetting in the case of a single target [9].

In this paper we analyze the effects of finite return times and refractory periods on directed search processes with stochastic resetting. For simplicity, we assume that the particle moves with constant speed v_+ in the search phase rather than switching between a moving state and a stationary state as in [7]. (This simplifies the analysis without affecting the main results of the paper.) We assume that there exists a 1D array of N contiguous targets of size l with $Nl = L$. These could represent neighboring synaptic targets along the axon or dendrite of a neuron (Fig. 1) or a line of target cells in the case of cytoneme-based transport (Fig. 2). We then consider two different search scenarios. The first (model A) consists of bounded search on the interval $[0, L]$, where L is the length of the target array, with a refractory (sticky) boundary at $x = 0$

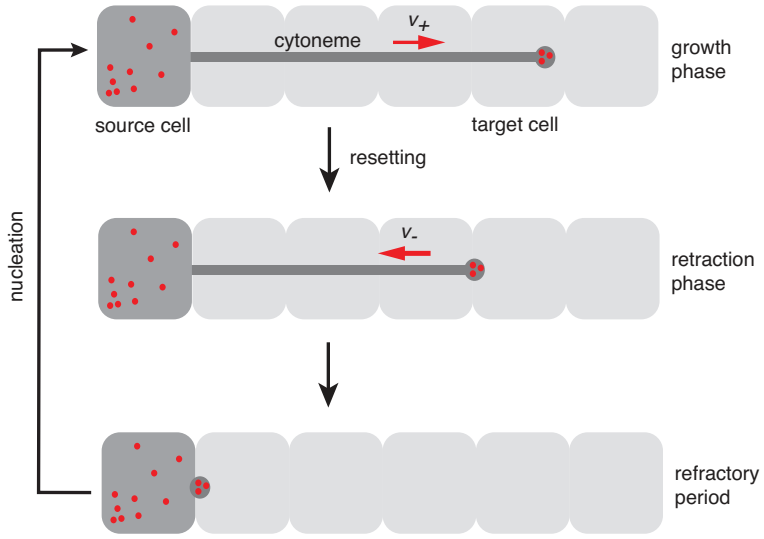

Figure 2: Search-and-capture model of cytoneme-based transport. A cytoneme grows along the surface of a 1D array of target cells at a speed v_+ until it eventually forms a contact with one of the cells and delivers the morphogen at its tip. Prior to finding a target, the cytoneme may randomly switch to a retraction phase (resetting) and return to the origin at speed v_-. After a refractory period (nucleation waiting time), a new cytoneme starts to grow.

and a reflecting boundary at $x = L$. The latter boundary condition means that if the particle reaches the end of the domain, then it returns to the origin at constant speed. The second scenario (model B) involves partially bounded search on the half-line with a refractory boundary at $x = 0$. In contrast to model A, in the absence of resetting there is a non-zero probability that the particle moves beyond $x = L$ without being captured by a target, which implies that the MFPT to capture is infinite. This is analogous to the directed search process with multiple targets considered in [7].

The structure of the paper is as follows. The search-and-capture model is introduced in section 2. In order to develop the analysis of stochastic resetting with delays, we first consider the simpler problem of directed search on the half-line with a single target (section 3). In section 4, we extend the analysis to determine the splitting probabilities and MFPTs for the particle to be captured by one of multiple targets. We show that models A and B have the same splitting probabilities but different MFPTs. In section 5 we explore the dependence of the splitting probabilities and conditional MFPTs on various model parameters, including the speeds of the search phase (v_+) and return phase (v_-), and the resetting rate r. We find that increasing the resetting rate r increases (reduces) the splitting probability for proximal (distal) targets. On the other hand, the MFPTs for model A are monotonically increasing functions of r, whereas the MFPTs of model B are non-monotonic with a minimum at an optimal resetting rate. We also show how increasing the search speed leads to a more uniform distribution of statistical quantities across the target array. Finally, in section 6 we analyze the accumulation of resources in the targets following multiple round of search-and-capture events by extending the queueing theory of [9] to multiple targets.

2. Directed search-and-capture model

Consider a particle moving ballistically on the finite interval $x \in [0, L]$. Suppose that the particle can exist in one of two discrete states: a right-moving (anterograde) state with speed v_+ or a left-moving (retrograde) state with speed v_-. The particle can undergo the state transition $v_+ \to v_-$ at a resetting rate r, after which it returns to the origin. At the origin the particle enters a refractory state for an exponentially distributed waiting time with rate η, prior to re-entering the domain in the anterograde state. Finally, we impose a reflecting boundary condition at $x = L$, such that if the particle reaches the end $x = L$ then it switches to the retrograde state and returns to the origin. The different states of the particle are shown schematically in Fig. 3. In this paper we are interested in the first passage time problem for the particle to find one of N contiguous targets of size l with $Nl = L$. Therefore, we introduce the additional assumption that the particle can be absorbed anywhere in the domain $[0, L]$ at a rate κ.

Let $p_n(x, t)$ be the probability density that at time t the particle is at $X(t) = x$ and in either the anterograde state ($n = +$) or the retrograde state ($n = -$). Similarly, let $P_0(t)$ denote the probability that the particle is in the refractory state at time t. The corresponding Chapman-Kolmogorov (CK) equation take the form

Model A

$$\frac{\partial p_+}{\partial t} = -v_+ \frac{\partial p_+}{\partial x} - r p_+ - \kappa p_+, \quad x \in (0, L), \tag{2.1a}$$

$$\frac{\partial p_-}{\partial t} = v_- \frac{\partial p_-}{\partial x} + r p_+, \tag{2.1b}$$

$$\frac{dP_0}{dt} = v_- p_-(0, t) - \eta P_0(t), \tag{2.1c}$$

together with the boundary conditions

$$v_+ p_+(0, t) = \eta P_0(t), \quad v_+ p_+(L, t) = v_- p_-(L, t). \tag{2.1d}$$

We assume that the particle starts in the anterograde state at $x = 0$. (Note that equation (2.1c) and the boundary condition at $x = 0$ are mathematically identical to so-called sticky boundary conditions used in models of bidirectional transport and

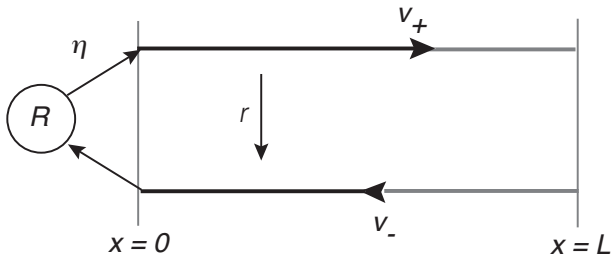

Figure 3: Schematic representation of particle states: anterograde state with speed v_+, retrograde state with speed v_- and a refractory state R. The refractory period τ is generated by an exponential waiting time density $\psi(\tau) = \eta e^{-\eta\tau}$, and r denotes the resetting rate.

microtubular catastrophes [18, 24, 6].) The probability $P_k(t)$ that the particle is captured by the k-th target at time t is

$$\frac{dP_k}{dt} = \kappa \int_{(k-1)l}^{kl} p_+(x,t)dx, \quad k = 1, \ldots, N. \tag{2.2}$$

Summing equations (2.1*a*) and (2.1*b*) and then integrating with respect to x over the interval $[0, L]$ shows that

$$\frac{d}{dt}\int_0^L p(x,t)dx = -\left[v_+p_+(x,t) - v_-p_-(x,t)\right]\Big|_0^L - \kappa \int_0^L p_+(x,t)dx,$$

where $p = p_+ + p_-$. Given the boundary conditions (2.1*d*), it follows that

$$\frac{d}{dt}\int_0^L p(x,t)dx + \sum_{k=0}^{N} \frac{dP_k}{dt} = 0,$$

which ensures conservation of total probability over all events, that is

$$\int_0^L p(x,t)dx + \sum_{k=0}^{N} P_k(t) = 1. \tag{2.3}$$

An illustration of a sample trajectory of the particle prior to capture is shown in Fig. 4.

We also consider a slightly modified version of model A, in which there is no reflecting boundary at $x = L$. Instead, the particle can continue beyond the array of targets until it resets and switches to the return phase. Now equations (2.1*a*)–(2.1*d*) become

Model B

$$\frac{\partial p_+}{\partial t} = -v_+\frac{\partial p_+}{\partial x} - rp_+ - \kappa H(L-x)p_+, \quad x \in (0,\infty), \tag{2.4a}$$

$$\frac{\partial p_-}{\partial t} = v_-\frac{\partial p_-}{\partial x} + rp_+, \quad x \in (0,\infty), \tag{2.4b}$$

$$\frac{dP_0}{dt} = v_-p_-(0,t) - \eta P_0(t), \quad v_+p_+(0,t) = \eta P_0(t), \tag{2.4c}$$

where $H(x)$ is the Heaviside function. There is a major difference between the two models in the absence of resetting. In the former case (model A), the particle is captured by one of the targets with probability one when $r = 0$, which is a consequence of the reflecting boundary condition at $x = L$. On the other hand, in the latter case (model B) there is a nonzero probability of passing beyond the target array and thus failing to be captured by any target, analogous to the model analyzed in [7]. This will lead to differences in how the conditional MFPTs vary with the resetting rate (see section 5).

3. MFPT for a single target

We begin our analysis by considering the simpler problem of a particle moving rightward on the half-line at a constant speed v_+ (as in model B), with a single target at a fixed location $X^* > 0$ and resetting to the origin. If the particle is within a distance l of the target, $l \leq X^*$, then the particle can detect or, equivalently, be absorbed by the target at a rate κ.

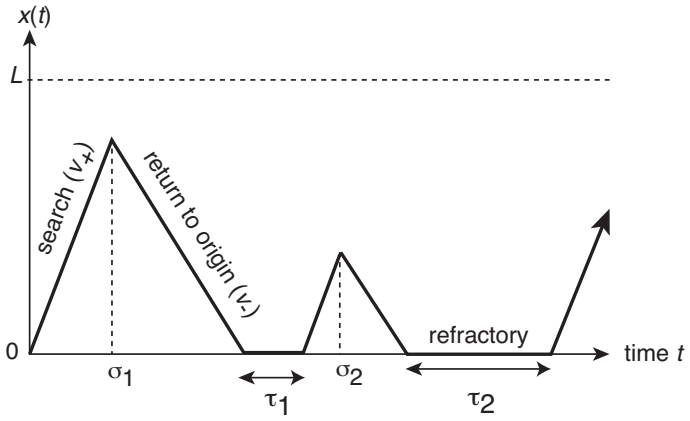

Figure 4: Directed search-and-capture model with stochastic resetting. Illustration of a sample trajectory of a particle prior to capture by a target in the domain $[0, L]$. Resetting events (indicated by the times σ_1, σ_2) are Poissonian with a rate r. The refractory periods τ_1, τ_2 are generated by an exponential waiting time density $\psi(\tau) = \eta \mathrm{e}^{-\eta\tau}$ with rate η. In model A there is a reflecting boundary at $x = L$, whereas the particle can continue beyond the array in model B.

3.1. MFPT with instantaneous resetting

In the case of instantaneous resetting, we have

$$\frac{\partial p_+}{\partial t} = -v_+ \frac{\partial p_+}{\partial x} - \kappa\chi(x - X^*)p_+ - rp_+ + r\delta(x). \tag{3.1}$$

Here $\chi(x)$ is an indicator function: $\chi(x) = 1$ if $|x| < l$ and is zero otherwise. Let $Q_r(x_0, t)$ denote the survival probability that the particle hasn't been absorbed by the target up to time t, having started at x_0 :

$$Q_r(x_0, t) = \int_0^\infty p_+(x, t|x_0, 0)dx, \tag{3.2}$$

where we have made the initial condition explicit. In particular, we set $Q_r(t) = Q_r(0, t)$. The MFPT T_r to be absorbed by the target can be expressed in terms of the survival probability according to

$$T_r = -\int_0^\infty t\frac{dQ_r(t)}{dt}dt = \int_0^\infty Q_r(t)dt. \tag{3.3}$$

One now observes that Q_r can be related to the survival probability without resetting, Q_0, using a last renewal equation [17]:

$$Q_r(x_0, t) = \mathrm{e}^{-rt}Q_0(x_0, t) + r\int_0^t Q_0(t')Q_r(x_0, t - t')\mathrm{e}^{-rt'}dt'.$$

The first term on the right-hand side represents trajectories with no resettings. The integrand in the second term is the contribution from trajectories that last reset at time $t-t'$, and consists of the product of the survival probability starting from $x = x_0$ with resetting up to time $t-t'$ and the survival probability starting from $x = 0$ without

any resetting for the time interval of duration t'. Since we have a convolution, it is natural to introduce the Laplace transform

$$\widetilde{Q}_r(x_0,s)=\int_0^\infty Q_r(x_0,t)\mathrm{e}^{-st}dt.$$

Laplace transforming the last renewal equation and rearranging gives [17]

$$\widetilde{Q}_r(x_0,s)=\frac{\widetilde{Q}_0(x_0,r+s)}{1-r\widetilde{Q}_0(r+s)}. \tag{3.4}$$

Substituting into equation (3.3) with $x_0=0$ then shows that the MFPT to reach the target is

$$T_r=\widetilde{Q}_r(0)=\frac{\widetilde{Q}_0(r)}{1-r\widetilde{Q}_0(r)}. \tag{3.5}$$

The Laplace transform of $Q_0(x_0,t)$ can be determined by Laplace transforming the corresponding backward master equation without resetting, which takes the form

$$-1=v_+\frac{\partial\widetilde{Q}_0(x_0,s)}{\partial x_0}-s\widetilde{Q}_0(x_0,s)-\kappa\chi(x_0-X^*)\widetilde{Q}_0(x_0,s).$$

This equation can be solved separately in the three domains $0<x_0<X^*-l$, $X^*-l<x_0<X^*+l$ and $X^*+l<x_0<\infty$, after imposing continuity across the boundaries at $x_0=X^*\pm l$ together with the condition $Q_0(x_0,t)=1$ for $x_0\geq X^*+l$. The latter implies that $\widetilde{Q}_0(X^*+l,s)=1/s$. The final result after setting $x_0=0$ is

$$\begin{aligned}\widetilde{Q}_0(s)=&\frac{1}{s}\left(1-\mathrm{e}^{-g_0(s)(X^*-l)}\right)\\&+\mathrm{e}^{-g_0(s)(X^*-l)}\left[\frac{1}{s}\mathrm{e}^{-2lg_\kappa(s)}+\frac{1}{s+\kappa}\left(1-\mathrm{e}^{-2lg_\kappa(s)}\right)\right],\end{aligned} \tag{3.6}$$

with $g_\kappa(s)=(s+\kappa)/v_+$. Note that

$$\lim_{t\to\infty}Q_0(t)=\lim_{s\to0}s\widetilde{Q}_0(s)=\mathrm{e}^{-(X^*+l)\kappa/v_+}.$$

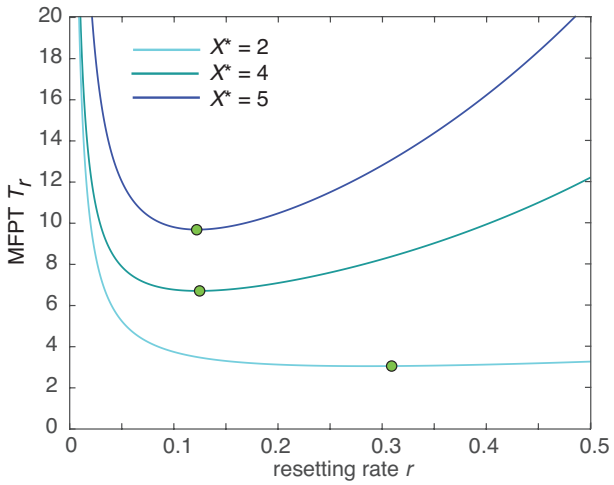

Figure 5: Plot of T_r as a function of the resetting rate r for various target locations X^* and $v_+=\kappa=l=1$. Green dots indicate optimal resetting rates.

That is, there is a nonzero probability that the particle fails to find the target, which is equal to the probability that it moves beyond the target without being absorbed. It follows that the MFPT is infinite. On the other hand,

$$\lim_{t\to\infty} Q_r(t) = \lim_{s\to 0} s\widetilde{Q}_r(s) = 0,$$

which implies that the particle is absorbed by the target with probability one. Stochastic resetting also renders the corresponding MFPT to be finite, as illustrated in Fig. 5. As found in previous studies of search processes with stochastic resetting, there exists an optimal resetting rate that minimizes the MFPT.

We now extend the standard renewal equation (3.4) in order to take into account refractory periods and finite return times. Since they affect the MFPT in an additive fashion, we consider them separately, starting with refractory periods (see also [16]). Throughout we take $x_0 = 0$. Note that a more general expression for the MFPT of a search process with stochastic resetting and delays has recently been derived in Refs. [27, 3].

3.2. Refractory periods

Let $\psi(\tau)$ denote the waiting time density for the refractory period following each return to the origin, with a finite mean $\overline{\tau}$. The generalized renewal equation takes the form

$$\begin{aligned} Q_r(t) = {} & \mathrm{e}^{-rt}Q_0(t) + r\int_0^t (1-\Psi(\sigma))\mathrm{e}^{-r(t-\sigma)}Q_0(t-\sigma)d\sigma \\ & + r\int_0^t Q_0(t')\mathrm{e}^{-rt'}\left[\int_0^{t-t'}\psi(\tau)Q_r(t-t'-\tau)d\tau\right]dt'. \end{aligned} \tag{3.7}$$

The first term on the right-hand side represents trajectories with no resettings, and the second term sums over all trajectories that first reset at some time $t-\sigma$, $0 \le \sigma \le t$ and are still in the refractory state at time t. The probability of remaining refractory for a period t is $1-\Psi(t)$ with

$$\Psi(t) = \int_0^t \psi(\sigma)d\sigma.$$

The third term is the contribution from trajectories that last reset at time $t-t'-\sigma$, spent a time σ in the refractory state, and then exited the refractory state at time $t-t'$ without any further resettings. Laplace transforming equation (3.7), we have

$$\widetilde{Q}_r(s) = \widetilde{Q}_0(r+s) + r\frac{1-\widetilde{\psi}(s)}{s}\widetilde{Q}_0(r+s) + r\widetilde{Q}_0(r+s)\widetilde{\psi}(s)\widetilde{Q}_r(s),$$

which can be rearranged to yield

$$\widetilde{Q}_r(s) = \frac{\widetilde{Q}_0(r+s)\left[1+\dfrac{r(1-\widetilde{\psi}(s))}{s}\right]}{1-r\widetilde{Q}_0(r+s)\widetilde{\psi}(s)}. \tag{3.8}$$

Taking the limit $s\to 0$ in equation (3.8) using $\widetilde{\psi}(0)=1$ and

$$\lim_{s\to 0}\frac{1-\psi(s)}{s} = -\psi'(0) = \int_0^\infty \tau\psi(\tau)d\tau \equiv \overline{\tau},$$

we thus find that the MFPT in the presence of a refractory period is

$$T_r = \frac{\widetilde{Q}_0(r)[1+r\overline{\tau}]}{1-r\widetilde{Q}_0(r)}. \tag{3.9}$$

This reduces to equation (3.5) in the absence of a refractory period.

3.3. Finite return times

Rather than a refractory period, suppose that the particle returns to the origin at a speed v_- following each resetting event. Equation (3.1) becomes

$$\frac{\partial p_+}{\partial t} = -v_+\frac{\partial p_+}{\partial x} - \kappa\chi(x-X^*)p_+ - rp_+, \tag{3.10a}$$

$$\frac{\partial p_-}{\partial t} = v_-\frac{\partial p_-}{\partial x} + rp_+, \quad x\in(0,\infty), \tag{3.10b}$$

$$v_+p_+(0,t) = v_-p_-(0,t). \tag{3.10c}$$

In order to link up with other work [16, 26], we briefly consider the steady-state density on the half-line $x\in[0,\infty)$ in the absence of any targets ($\kappa=0$). Adding equations (3.10*a*) and (3.10*b*) after setting time derivatives to zero, and imposing the reflecting boundary condition shows that $v_+p_+(x) = v_-p_-(x)$. Next, solving equation (3.10*a*) gives

$$p_+(x) = p_+(0)\mathrm{e}^{-rx/v_+},$$

with the constant $p_+(0)$ determined from the normalization condition

$$1 = \int_0^\infty [p_+(x)+p_-(x)]dx = \left(1+\frac{v_+}{v_-}\right)p_+(0)\int_0^\infty \mathrm{e}^{-ry/v_+}dy.$$

Hence,

$$p_+(x) = \frac{v_-}{v_++v_-}\frac{r}{v_+}\mathrm{e}^{-rx/v_+}. \tag{3.11}$$

In the case of instantaneous reset ($v_-\to\infty$), we obtain the familiar steady-state

$$p_\infty(x) = \frac{r}{v_+}\mathrm{e}^{-rx/v_+}. \tag{3.12}$$

Consistent with the more general results obtained in [16, 26], the steady-state density is equal to the density $p_\infty(x)$ multiplied by the mean fraction of time spent in the ballistic state.

Turning to the calculation of the MFPT, we have to write down the appropriate generalization of the renewal equation (3.4):

$$\begin{aligned} Q_r(t) = \mathrm{e}^{-rt}Q_0(t) + r\int_0^{t/\xi_+}\mathrm{e}^{-r(t-\sigma)}Q_0(t-\sigma)d\sigma \\ + \int_0^t Q_0(t')r\mathrm{e}^{-rt'}\left[\int_0^{(t-t')/\xi_-} Q_r(t-t'-\sigma\xi_-)r\mathrm{e}^{-r\sigma}d\sigma\right]dt', \end{aligned} \tag{3.13}$$

where

$$\xi_+ = \frac{v_++v_-}{v_+}, \quad \xi_- = \frac{v_+}{v_-}.$$

As in equation (3.4), the first term on the right-hand side represents trajectories with no resettings. The second term sums over all trajectories that first reset at some time

$t-\sigma$, $0 \leq \sigma \leq t/\xi_+$ and are still in the process of returning to the origin. Since the particle has been in the ballistic state for time $t-\sigma$, it has traveled a distance $v_+(t-\sigma)$, which means that

$$\sigma \leq \frac{v_+}{v_-}(t-\sigma).$$

Rearranging this equation yields the constraint that $\sigma \leq t/\xi_+$. The third term is the contribution from trajectories whose last reset occurred at time $t-t'-v_+\sigma/V$, where σ is the time spent in the ballistic state prior to resetting, after which the particle takes a time $v_+\sigma/v_-$ to return to the origin, and then an additional time t' in the ballistic state without any further resettings. We also require

$$\sigma\frac{v_+}{v_-} \leq (t-t'),$$

which yields the constraint $\sigma \leq (t-t')/\xi_-$.

We now Laplace transform the various terms in equation (3.13). First, set

$$A(t) := \int_0^{t/\xi_+} \mathrm{e}^{-r(t-\sigma)}Q_0(t-\sigma)d\sigma = \int_{t/\xi}^{t} \mathrm{e}^{-r\sigma}Q_0(\sigma)d\sigma,$$

with $\xi^{-1} = 1-\xi_+^{-1}$. It follows that

$$\frac{dA}{dt} = Q_0(t)\mathrm{e}^{-rt} - \xi^{-1}Q_0(t/\xi)\mathrm{e}^{-rt/\xi}.$$

Laplace transforming this equation with $A(0)=0$ yields

$$\widetilde{A}(s) = \frac{\widetilde{Q}_0(r+s) - \widetilde{Q}_0(r+\xi s)}{s}. \tag{3.14}$$

Next, let

$$B(t) := \int_0^{t/\xi_-} Q_r(t-\sigma\xi_-)r\mathrm{e}^{-r\sigma}d\sigma = \xi_-^{-1}\int_0^t Q_r(t-\tau)r\mathrm{e}^{-r\tau/\xi_-}d\tau.$$

Hence,

$$\widetilde{B}(s) = \frac{\widetilde{Q}_r(s)}{s\xi_- + r}. \tag{3.15}$$

Finally, Laplace transforming equation (3.13) using equations (3.14) and (3.15) gives

$$\widetilde{Q}_r(s) = \widetilde{Q}_0(r+s) + r\left[\frac{\widetilde{Q}_0(r+s) - \widetilde{Q}_0(r+\xi s)}{s}\right] + \frac{r^2}{s\xi_- + r}\widetilde{Q}_0(r+s)\widetilde{Q}_r(s),$$

which can be rearranged to yield

$$\widetilde{Q}_r(s) = \frac{\widetilde{Q}_0(r+s) + r\left[\widetilde{Q}_0(r+s) - \widetilde{Q}_0(r+\xi s)\right]/s}{1 - r^2\widetilde{Q}_0(r+s)/(r+s\xi_-)}. \tag{3.16}$$

Taking the limit $s \to 0$ in equation (3.16) using

$$\lim_{s\to 0}\frac{\widetilde{Q}_0(r+s) - \widetilde{Q}_0(r+\xi s)}{s} = (1-\xi)\widetilde{Q}_0'(r) = -\frac{v_+}{v_-}\widetilde{Q}_0'(r),$$

we find that the MFPT in the presence of finite return times is

$$T_r = \frac{\widetilde{Q}_0(r) - r\frac{v_+}{v_-}\widetilde{Q}_0'(r),}{1 - r\widetilde{Q}_0(r)}. \tag{3.17}$$

Again this reduces to equation (3.5) in the limit $v_- \to \infty$ (instantaneous resetting). Finally, equations (3.9) and (3.17) show that the combined effect of refractory periods and finite returns times is an MFPT of the form

$$T_r = \frac{\widetilde{Q}_0(r) + r\overline{\tau}\widetilde{Q}_0(r) - r\frac{v_+}{v_-}\widetilde{Q}_0'(r),}{1 - r\widetilde{Q}_0(r)}. \tag{3.18}$$

Since $\widetilde{Q}_0(r) > 0$ and $\widetilde{Q}_0'(r) < 0$ we see that both types of delay increase the MFPT, as one would expect. This is consistent with the more general result obtained in [27, 3].

3.4. Alternative renewal method

We now describe an alternative renewal method for calculating MFPTs in the presence of delays, which is based on conditioning the first passage time on whether or not the particle resets at least once. This approach was previously applied to the search-and-capture model of cytoneme-based morphogen transport [6], and has recently been used to derive a general expression for a search process with stochastic resetting and delays [27]. We will extend this method to multiple targets in section 4, following along the lines of [8].

The basic idea is to exploit the fact that resetting eliminates any memory of previous search stages. Introduce the discrete random variable $K(t) \in \{0, 1\}$, which indicates whether the particle has been captured by the target ($K(t) = 1$) or is still free ($K(t) = 0$) in the time interval $[0, t]$. Consider the following set of first passage times;

$$\begin{aligned}
\mathcal{T} &= \inf\{t > 0; X^* - l \leq X(t) \leq X^* + l,\ K(t) = 1\},\\
\mathcal{S} &= \inf\{t > 0; X(t) = 0,\ K(t) = 0\},\\
\mathcal{R} &= \inf\{t > 0; X^* - l \leq X(t + \mathcal{S} + \mathcal{N}) \leq X^* + l,\ K(t + \mathcal{S} + \mathcal{N}) = 1\}.
\end{aligned}$$

Here $\mathcal{T}$ is the FPT for finding the target irrespective of the number of resettings, $\mathcal{S}$ is the FPT for the first resetting and return to the origin given that the particle is still free, $\mathcal{N}$ is the first refractory period, and $\mathcal{R}$ is the FPT for finding the target given that at least one resetting has occurred. Next we introduce the sets

$$\Omega = \{\mathcal{T} < \infty\}, \quad \Gamma = \{\mathcal{S} < \mathcal{T} < \infty\} \subset \Omega.$$

That is, Ω is the set of all events for which the particle is eventually absorbed by the target (which has measure one), and Γ is the subset of events in Ω for which the particle resets at least once. It immediately follows that

$$\Omega\backslash\Gamma = \{\mathcal{T} < \mathcal{S} = \infty\}.$$

In other words, $\Omega\backslash\Gamma$ is the set of all events for which the particle is captured by the target without any resetting. We now use a probabilistic argument to calculate the MFPT $T_r = \mathbb{E}[\mathcal{T}]$ in the presence of resetting ($r > 0$).

Consider the decomposition

$$\mathbb{E}[\mathcal{T}] = \mathbb{E}[\mathcal{T}1_{\Omega\backslash\Gamma}] + \mathbb{E}[\mathcal{T}1_{\Gamma}]. \tag{3.19}$$

The first expectation on the right-hand side can be evaluated by noting that it is the MFPT for capture by the target without any resetting, and the probability density for such an event is $-\mathrm{e}^{-r\tau}\partial_t Q_0(t)$. Hence,

$$\mathbb{E}[\mathcal{T}1_{\Omega\backslash\Gamma}] = -\int_0^\infty \tau \mathrm{e}^{-r\tau}\frac{\partial Q_0(\tau)}{\partial \tau}d\tau = \left(1 + r\frac{d}{dr}\right)\widetilde{Q}_0(r), \tag{3.20}$$

The second expectation can be further decomposed as

$$\begin{aligned}\mathbb{E}[\mathcal{T}1_\Gamma] &= \mathbb{E}[(\mathcal{S}+\mathcal{N}+\mathcal{R})1_\Gamma] = \mathbb{E}[\mathcal{S}1_\Gamma] + \overline{\tau}\mathbb{P}[\Gamma] + \mathbb{E}[\mathcal{R}1_\Gamma] \\ &= \mathbb{E}[\mathcal{S}1_\Gamma] + (\overline{\tau}+T_r)\mathbb{P}[\Gamma]. \end{aligned} \tag{3.21}$$

Here $\mathbb{E}[\mathcal{N}] = \overline{\tau}$ is the mean refractory period, and we have used the result $\mathbb{E}[\mathcal{R}1_\Gamma] = T_r\mathbb{P}[\Gamma]$. The latter follows from the fact that return to the origin restarts the stochastic process without any memory.

In order to calculate $\mathbb{E}[\mathcal{S}1_\Gamma]$, it is necessary to incorporate the time to return to the origin following the first return event. The first resetting occurs with probability $re^{-r\tau}Q_0(\tau)d\tau$ in the interval $[\tau, \tau+d\tau]$. At time τ the particle is at position $v_+\tau$ and thus takes an additional time $v_+\tau/v_-$ to return to $x=0$. We thus find

$$\mathbb{E}[\mathcal{S}1_\Gamma] = \int_0^\infty re^{-r\tau}\tau\left(1+\frac{v_+}{v_-}\right)Q_0(\tau)d\tau = -r\left(1+\frac{v_+}{v_-}\right)\frac{d}{dr}\widetilde{Q}_0(r). \tag{3.22}$$

Moreover, from the definitions of the first passage times and the effect of resetting,

$$\mathbb{P}[\Gamma] = \mathbb{P}[\mathcal{S}<\infty]\mathbb{P}[\mathcal{R}<\infty], \tag{3.23}$$

with $\mathbb{P}[\mathcal{R}<\infty]=1$ and

$$\mathbb{P}[\mathcal{S}<\infty] = \int_0^\infty re^{-r\tau}Q_0(\tau)d\tau = r\widetilde{Q}_0(r). \tag{3.24}$$

Combining equations (3.20)–(3.24) yields the implicit equation

$$T_r = \left(1+r\frac{d}{dr}\right)\widetilde{Q}_0(r) + r\overline{\tau}\widetilde{Q}_0(r) - r\left(1+\frac{v_+}{v_-}\right)\frac{d}{dr}\widetilde{Q}_0(r) + r\widetilde{Q}_0(r)T_r. \tag{3.25}$$

Rearranging this equation then recovers the general result (3.18). In the following we take $\psi(\tau)$ to be an exponential waiting time density with rate η so that $\overline{\tau}=\eta^{-1}$.

4. Splitting probabilities and conditional MFPTs for multiple targets

We now wish to extend the above probabilistic renewal method to calculate the splitting probability $\pi_k^{(r)}$ that a particle evolving according to model A or B in section 2 is eventually captured by the k-th target,

$$\pi_k^{(r)} = \lim_{t\to\infty} P_k(t), \quad \sum_{k=1}^N \pi_k^{(r)} = 1, \tag{4.1}$$

and the corresponding conditional mean first passage time $T_k^{(r)}$. This will generate expressions for $\pi_k^{(r)}$ and $T_k^{(r)}$ in terms of statistical quantities for the search process without a return phase (no resetting nor reflection at $x=L$). Hence, the first step is to analyze target capture in the absence of a return phase, which means that if the particle reaches the end $x=L$ then it cannot be captured by any target.

4.1. Target capture without a return phase

Consider the splitting probability π_k and conditional MFPT T_k for the particle to be captured by the k-th target when $p_-(x,t)\equiv 0$ (no return phase), having started in the search phase at position $x=0$ at time $t=0$. The first step is to solve equation (2.1*a*) with $r=0$, which becomes

$$\frac{\partial p_+}{\partial t} = -v_+\frac{\partial p_+}{\partial x} - \kappa p_+. \tag{4.2}$$

This has the explicit solution

$$p_+(x,t|0,0) = \delta(x - v_+ t)\mathrm{e}^{-\kappa t}, \quad 0 < t < \frac{L}{v_+}.$$

The probability flux into the k-th target is

$$J_k(t) = \kappa \int_{(k-1)l}^{kl} p_+(x,t|0,0)dx = \kappa \int_{(k-1)l}^{kl} \delta(x - v_+ t)\mathrm{e}^{-\kappa t}dx = \kappa \chi_k(t)\mathrm{e}^{-\kappa t}, \tag{4.3}$$

where $\chi_k(t) = 1$ if $\tau_{k-1} < t < \tau_k$ and zero otherwise, and we have set $\tau_k = kl/v_+$. Let $\mathcal{T}_k$ denote the FPT that the particle is captured by the k-th target, with $\mathcal{T}_k = \infty$ indicating that it is not captured. The splitting probability that the particle is captured by the k-th target is

$$\pi_k := \mathbb{P}[0 < \mathcal{T}_k < \infty] = \int_0^\infty J_k(y,t')dt' = \kappa \int_0^\infty \chi_k(t)\mathrm{e}^{-\kappa t} = \mathrm{e}^{-\kappa\tau_{k-1}} - \mathrm{e}^{-\kappa\tau_k}. \tag{4.4}$$

Here $\mathrm{e}^{-\kappa\tau_{k-1}}$ is the probability of reaching the k-th target without being captured by any upstream targets, so π_k is the probability that the particle is captured by the k-th target before passing to the $(k+1)$-th target. It follows that

$$\sum_{k=1}^{N} \pi_k = 1 - \mathrm{e}^{-\kappa L/v_+}, \tag{4.5}$$

where $\mathrm{e}^{-\kappa L/v_+}$ is the probability the particle reaches the end without being captured by any target in the array.

Given the splitting probability π_k, we define the corresponding conditional MFPT by

$$T_k = \mathbb{E}[\mathcal{T}_k|\mathcal{T}_k < \infty]. \tag{4.6}$$

In order to determine T_k, it is convenient to consider the probability $\Pi_k(t)$ that the particle is captured by the k-th target after time t:

$$\Pi_k(t) = \mathbb{P}[t < \mathcal{T}_k < \infty] = \int_t^\infty J_k(t')dt'. \tag{4.7}$$

Substituting for $J_k(t)$ using equation (4.3) gives

$$\Pi_k(t) = H(\tau_k - t)\left[\mathrm{e}^{-\kappa t} - \mathrm{e}^{-\kappa\tau_k}\right] + H(\tau_{k-1} - t)\left[\mathrm{e}^{-\kappa\tau_{k-1}} - \mathrm{e}^{-\kappa t}\right], \tag{4.8}$$

where $H(t)$ is the Heaviside function. Note that $\Pi_k(0) = \pi_k$, and the complementary probability $\Lambda_k(t)$ that the particle is captured by the k-th target before time t is

$$\Lambda_k(t) = \int_0^t J_k(t')dt' = \int_0^\infty J_k(t')dt' - \int_t^\infty J_k(t')dt' = \pi_k - \Pi_k(t). \tag{4.9}$$

The conditional MFPT can now be written as

$$T_k = \int_0^\infty \frac{\Pi_k(t)}{\pi_k}dt = \frac{\widetilde{\Pi}_k(0)}{\pi_k},$$

where $\widetilde{\Pi}_k(s)$ is the Laplace transform of $\Pi_k(\tau)$:

$$\begin{aligned}\widetilde{\Pi}_k(s) = {} & \frac{1}{s+\kappa}\left(1 - \mathrm{e}^{-(s+\kappa)\tau_k}\right) - \frac{1}{s}\left(1 - \mathrm{e}^{-s\tau_k}\right)\mathrm{e}^{-\kappa\tau_k} \\ & - \frac{1}{s+\kappa}\left(1 - \mathrm{e}^{-(s+\kappa)\tau_{k-1}}\right) + \frac{1}{s}\left(1 - \mathrm{e}^{-s\tau_{k-1}}\right)\mathrm{e}^{-\kappa\tau_{k-1}}.\end{aligned} \tag{4.10}$$

Hence,

$$\pi_k T_k = \frac{\pi_k}{\kappa} + \tau_k \mathrm{e}^{-\kappa\tau_k} - \tau_{k-1}\mathrm{e}^{-\kappa\tau_{k-1}}. \tag{4.11}$$

4.2. Target capture with a return phase: probabilistic renewal method

In order to incorporate the effects of stochastic resetting (or reflection at $x = L$ in model A) and delays, we introduce the discrete random variable $K(t) \in \{0, 1, \ldots, N\}$, which indicates whether the particle has been captured by the k-th target ($K(t) = k$, $k \neq 0$) or has not been absorbed by any target ($K(t) = 0$) in the time interval $[0, t]$. Consider the following set of first passage times;

$$\begin{aligned}\mathcal{T}_k &= \inf\{t > 0; (k-1)l \leq X(t) \leq kl, K(t) = k\},\\ \mathcal{S} &= \inf\{t > 0; X(t) = 0, K(t) = 0\},\\ \mathcal{R}_k &= \inf\{t > 0; (k-1)l \leq X(t + \mathcal{S} + \mathcal{N}) \leq kl, K(t + \mathcal{S} + \mathcal{N}) = k\}.\end{aligned}$$

Here $\mathcal{T}_k$ is the FPT for finding the k-th target irrespective of the number of return phases, $\mathcal{S}$ is the FPT for the first return to the origin given that no target has captured the particle, $\mathcal{N}$ is the first refractory period, and $\mathcal{R}_k$ is the FPT for finding the k-th target given that at least one return phase has occurred. Next we introduce the sets

$$\Omega_k = \{\mathcal{T}_k < \infty\}, \quad \Gamma_k = \{\mathcal{S} < \mathcal{T}_k < \infty\} \subset \Omega_k,$$

where Ω_k is the set of all events for which the particle is eventually absorbed by the k-th target, and Γ_k is the subset of events in Ω_k for which the particle returns to the origin at least once. It immediately follows that

$$\Omega_k \backslash \Gamma_k = \{\mathcal{T}_k < \mathcal{S} = \infty\}.$$

In other words, $\Omega_k \backslash \Gamma_k$ is the set of all events for which the particle is captured by the k-th target without any returns to the origin via resetting (or reflection at $x = L$ in the case of model A). We now generalize the probabilistic approach of section 3.4 to calculate the splitting probability $\pi_k^{(r)}$ and MFPT $T_k^{(r)}$ in the presence of resetting ($r > 0$).

The splitting probability $\pi_k^{(r)}$ can be decomposed as

$$\pi_k^{(r)} := \mathbb{P}[\Omega_k] = \mathbb{P}[\Omega_k \backslash \Gamma_k] + \mathbb{P}[\Gamma_k]. \tag{4.12}$$

We note that the probability that the particle is captured by the k-th target in the interval $[\tau, \tau + d\tau]$ without any returns to the origin is $\mathrm{e}^{-r\tau} J_k(\tau) d\tau$ with $J_k(\tau)$ given by equation (4.3). Hence,

$$\begin{aligned}\mathbb{P}[\Omega_k \backslash \Gamma_k] &= \int_0^\infty \mathrm{e}^{-r\tau} J_k(\tau) d\tau = -\int_0^\infty \mathrm{e}^{-r\tau} \frac{d\Pi_k(\tau)}{d\tau} d\tau\\ &= -r\widetilde{\Pi}_k(r) + \pi_k = r\widetilde{\Lambda}_k(r).\end{aligned} \tag{4.13}$$

Next, from the definitions of the first passage times, we have

$$\mathbb{P}[\Gamma_k] = \mathbb{P}[\mathcal{S} < \infty]\mathbb{P}[\mathcal{R}_k < \infty], \tag{4.14}$$

and memoryless return to the origin implies that $\mathbb{P}[\mathcal{R}_k < \infty] = \pi_k^{(r)}$. In the case of model B

$$\begin{aligned}\mathbb{P}[\mathcal{S} < \infty] &= \int_0^\infty r\mathrm{e}^{-r\tau} \left[1 - \sum_{k=1}^N \Lambda_k(\tau)\right] d\tau\\ &= 1 - r\sum_{k=1}^N \widetilde{\Lambda}_k(r) = r\sum_{k=1}^N \widetilde{\Pi}_k(r) + \mathrm{e}^{-\kappa L/v_+}.\end{aligned} \tag{4.15}$$

We have used the fact that the probability of first switching to the shrinking phase in the time interval $[\tau, \tau + d\tau]$ is equal to the product of the reset probability $r\mathrm{e}^{-r\tau} d\tau$

and the probability $1-\sum_k \Lambda_k(\tau)$ that the particle hasn't been captured by a target up to time τ. The term $\mathrm{e}^{-\kappa L/v_+}$ in the final expression arises from the normalization condition (4.5), and is the probability that the particle reaches the end of the array at $x=L$, after which it continues in the anterograde state until the first reset. It turns out that $\mathbb{P}[\mathcal{S}<\infty]$ is the same for model A. Now we only integrate the resetting time over the interval $\tau\in[0,L/v_+]$, after which the particle returns to the origin with probability one:

$$\mathbb{P}[\mathcal{S}<\infty]=\int_0^{L/v_+} r\mathrm{e}^{-r\tau}\left[1-\sum_{k=1}^N\Lambda_k(\tau)\right]d\tau+\mathrm{e}^{-rL/v_+}\mathrm{e}^{-\kappa L/v_+}.$$

The second term on the right-hand side is the probability that it reaches the end of the array without resetting nor target capture. Using the fact that $\sum_{k=1}^N\Pi_k(t)=0$ for $t>L/v_+$, we have

$$\begin{aligned}\int_0^{L/v_+} r\mathrm{e}^{-r\tau}\left[1-\sum_{k=1}^N\Lambda_k(\tau)\right]d\tau&=\int_0^{L/v_+} r\mathrm{e}^{-r\tau}\left[\sum_{k=1}^N\Pi_k(\tau)+\mathrm{e}^{-\kappa L/v_+}\right]d\tau\\&=r\sum_{k=1}^N\widetilde{\Pi}_k(r)+\mathrm{e}^{-\kappa L/v_+}(1-\mathrm{e}^{-rL/v_+}),\end{aligned}$$

and we recover equation (4.15). Hence, for both models, equation (4.14) becomes

$$\mathbb{P}[\Gamma_k]=\pi_k^{(r)}\left[r\sum_{k=1}^N\widetilde{\Pi}_k(r)+\mathrm{e}^{-\kappa L/v_+}\right]. \tag{4.16}$$

Combining equations (4.13) and (4.16) yields the implicit equation

$$\pi_k^{(r)}=r\widetilde{\Lambda}_k(r)+\left[1-r\sum_{k=1}^N\widetilde{\Lambda}_k(r)\right]\pi_k^{(r)},$$

which on rearranging leads to the following result, which holds for both models:

$$\pi_k^{(r)}=\frac{r\widetilde{\Lambda}_k(r)}{r\sum_{l=1}^N\widetilde{\Lambda}_l(r)}=\frac{\pi_k-r\widetilde{\Pi}_k(r)}{1-r\sum_{l=1}^N\widetilde{\Pi}_l(r)-\mathrm{e}^{-\kappa L/v_+}}. \tag{4.17}$$

Summing both sides of equation (4.17) and using equation (4.5) implies that $\sum_{k=1}^N\pi_k^{(r)}=1$. In other words, in the presence of reset, the particle is captured by one of the targets with probability one. Finally, using the fact that

$$\lim_{r\to0}r\widetilde{\Pi}_k(r)=\Pi_k(\infty)=0,$$

we have

$$\lim_{r\to0}\pi_k^{(r)}=\frac{\pi_k}{1-\mathrm{e}^{-\kappa L/v_+}}=\widehat{\pi}_k.$$

Note that the splitting probability $\pi_k^{(r)}$ is independent of the values of the refractory rate η and the retrograde speed v_-. However, implicit in the calculation of $\pi_k^{(r)}$ is the assumption that $v_-,\eta>0$, otherwise resetting would not allow the particle to return to the origin and then escape from the refractory state in a finite time.

The conditional MFPT $\mathbb{E}[\mathcal{T}_k1_{\Omega_k}]=\pi_k^{(r)}T_k^{(r)}$ can be analyzed along similar lines to the splitting probability by introducing the decomposition

$$\mathbb{E}[\mathcal{T}_k1_{\Omega_k}]=\mathbb{E}[\mathcal{T}_k1_{\Omega_k\backslash\Gamma_k}]+\mathbb{E}[\mathcal{T}_k1_{\Gamma_k}]. \tag{4.18}$$

The first expectation can be evaluated by noting that it is the MFPT for capture by the k-th target without any resetting, and the probability density for such an event is $\mathrm{e}^{-r\tau}J_k(\tau)d\tau$. Hence,

$$\mathbb{E}[\mathcal{T}_k 1_{\Omega_k\backslash\Gamma_k}] = -\int_0^\infty \tau \mathrm{e}^{-r\tau}\frac{d\Pi_k(\tau)}{d\tau}d\tau = \left[1 + r\frac{d}{dr}\right]\widetilde{\Pi}_k(r). \tag{4.19}$$

The second expectation can be further decomposed as

$$\begin{aligned}\mathbb{E}[\mathcal{T}_k 1_{\Gamma_k}] &= \mathbb{E}[(\mathcal{S}+\widehat{\tau}+\mathcal{R}_k)1_{\Gamma_k}] = \mathbb{E}[\mathcal{S}1_{\Gamma_k}] + \frac{1}{\eta}\mathbb{P}[\Gamma_k] + \mathbb{E}[\mathcal{R}_k 1_{\Gamma_k}]\\ &= \mathbb{E}[\mathcal{S}1_{\Gamma_k}] + \left(\frac{1}{\eta} + T_k^{(r)}\right)\mathbb{P}[\Gamma_k],\end{aligned} \tag{4.20}$$

with $\mathbb{P}[\Gamma_k]$ given by equation (4.16). Again $\mathcal{N}$ denotes the random time spent in the refractory state at $x=0$ before switching back to the search phase, with $\mathbb{E}[\mathcal{N}] = \eta^{-1}$, and we have used the result $\mathbb{E}[\mathcal{R}_k 1_{\Gamma_k}] = T_k^{(r)}\mathbb{P}[\Gamma_k]$. The latter follows from the fact that return to the origin restarts the stochastic process without any memory.

In order to calculate $\mathbb{E}[\mathcal{S}1_{\Gamma_k}]$, it is necessary to incorporate the time to return to the origin following the first return event, and this will differ for models A and B. In the case of model A, the first return is initiated before reaching the end $x=L$ with probability $r\mathrm{e}^{-r\tau}\sum_k \Pi_k(\tau)d\tau$ in the interval $[\tau,\tau+d\tau]$. At time τ the particle is at position $v_+\tau$ and thus takes an additional time $v_+\tau/v_-$ to return to $x=0$. Alternatively, the particle reaches $x=L$ with probability $\mathrm{e}^{-\kappa L/v_+}$ after the time $\tau = L/v_+$ and then returns to the origin over a time interval equal to L/v_-. We thus find

$$\begin{aligned}\mathbb{E}[\mathcal{S}1_{\Gamma_k}] &= \pi_k^{(r)}\left\{\int_0^\infty r\mathrm{e}^{-r\tau}\left(\tau+\frac{v_+\tau}{v_-}\right)\left[\sum_{k=1}^N \Pi_k(\tau)\right]d\tau + \left(\frac{L}{v_+}+\frac{L}{v_-}\right)\mathrm{e}^{-\kappa L/v_+}\right\}\\ &= \pi_k^{(r)}\left\{\left(\frac{L}{v_+}+\frac{L}{v_-}\right)\mathrm{e}^{-\kappa L/v_+} - r\left(1+\frac{v_+}{v_-}\right)\left[\sum_{k=1}^N \frac{d\widetilde{\Pi}_k(r)}{dr}\right]\right\}.\end{aligned} \tag{4.21a}$$

We have used $\mathbb{P}[\mathcal{R}_k<\infty] = \pi_k^{(r)}$ and the fact that $\sum_{k=1}^N \Pi_k(\tau) = 0$ for $\tau > L/v_+$. On the other hand, in the case of model B resetting can occur any time after the particle passes beyond the array so that

$$\begin{aligned}\mathbb{E}[\mathcal{S}1_{\Gamma_k}] &= \pi_k^{(r)}\left\{\int_0^\infty r\mathrm{e}^{-r\tau}\left(\tau+\frac{v_+\tau}{v_-}\right)\left[\sum_{k=1}^N \Pi_k(\tau)\right]d\tau\right.\\ &\qquad \left. +\mathrm{e}^{-\kappa L/v_+}\int_{L/v_+}^\infty r\mathrm{e}^{-r\tau}\left(\tau+\frac{v_+\tau}{v_-}\right)d\tau\right\}\\ &= \left\{\left(1+\frac{v_+}{v_-}\right)\left(\frac{1}{r}+\frac{L}{v_+}\right)\mathrm{e}^{-(\kappa+r)L/v_+} - r\left(1+\frac{v_+}{v_-}\right)\left[\sum_{k=1}^N \frac{d\widetilde{\Pi}_k(r)}{dr}\right]\right\}\pi_k^{(r)}.\end{aligned} \tag{4.21b}$$

Combining equations (4.19) and (4.20) with either (4.21a) or (4.21b) yields an implicit equation of the form

$$\pi_k^{(r)}T_k^{(r)} = \left[1+r\frac{d}{dr}\right]\widetilde{\Pi}_k(r) + \left\{\mathcal{A} - r\left(1+\frac{v_+}{v_-}\right)\left[\sum_{k=1}^N \frac{d\widetilde{\Pi}_k(r)}{dr}\right]\right\}\pi_k^{(r)},$$

$$+\left(\frac{1}{\eta}+T_k^{(r)}\right)\pi_k^{(r)}\left[r\sum_{k=1}^{N}\widetilde{\Pi}_k(r)+\mathrm{e}^{-\kappa L/v_+}\right], \tag{4.22}$$

where

$$\mathcal{A}=\begin{cases}\left(\frac{L}{v_+}+\frac{L}{v_-}\right)\mathrm{e}^{-\kappa L/v_+} & \text{(model A)},\\ \left(1+\frac{v_+}{v_-}\right)\left(\frac{1}{r}+\frac{L}{v_+}\right)\mathrm{e}^{-(\kappa+r)L/v_+} & \text{(model B)}.\end{cases} \tag{4.23}$$

Rearranging equation (4.22) we obtain the following result for the conditional MFPT:

$$T_k^{(r)}=\frac{\mathbb{L}\widetilde{\Pi}_k(r)+\mathcal{B}\pi_k^{(r)}}{\pi_k^{(r)}\left[1-r\sum_{k=1}^{N}\widetilde{\Pi}_k(r)-\mathrm{e}^{-\kappa L/v_+}\right]}. \tag{4.24}$$

Here

$$\mathbb{L}\widetilde{\Pi}_k(r)=\left[1+r\frac{d}{dr}\right]\widetilde{\Pi}_k(r)-r\left(1+\frac{v_+}{v_-}\right)\left[\sum_{k=1}^{N}\frac{d\widetilde{\Pi}_k(r)}{dr}\right]\pi_k^{(r)}, \tag{4.25}$$

and

$$\mathcal{B}=\frac{1}{\eta}\left[r\sum_{k=1}^{N}\widetilde{\Pi}_k(r)+\mathrm{e}^{-\kappa L/v_+}\right]+\mathcal{A}. \tag{4.26}$$

The MFPTs for models A and B display very different behavior in the limit $r\to 0$. In particular, it is clear from equation (4.23) that for model B we have $\mathcal{A}\to\infty$ as $r\to 0$, which implies $T_k^{(r)}\to\infty$ as $r\to 0$. This reflects the fact that the MFPTs for model B are infinite in the absence of resetting. On the other hand, $\mathcal{A}$ is independent of r for model A, and we find

$$\lim_{r\to 0}T_k^{(r)}=\frac{1}{1-\mathrm{e}^{-\kappa L/v_+}}\left[\frac{\widetilde{\Pi}_k(0)\left[1-\mathrm{e}^{-\kappa L/v_+}\right]}{\pi_k}+\left[\frac{1}{\eta}+L\left(\frac{1}{v_+}+\frac{1}{v_-}\right)\right]\mathrm{e}^{-\kappa L/v_+}\right]. \tag{4.27}$$

This expression has an intuitive interpretation. In the limit $r\to 0$, the particle can only return to the origin by reflecting at the end $x=L$, which occurs with probability $\mathrm{e}^{-\kappa L/v_+}$ during one search phase. The first term in square brackets is the conditional MFPT without any returns to the origin, while the second term is the additional time taken to reach the end and return to the origin once before being captured. The Taylor expansion

$$\frac{1}{1-\mathrm{e}^{-\kappa L/v_+}}=1+\mathrm{e}^{-\kappa L/v_+}+\mathrm{e}^{-2\kappa L/v_+}+\ldots$$

generates an infinite sum over paths that return to the origin n times with probability $\mathrm{e}^{-n\kappa L/v_+}$.

5. Results

In this section we illustrate the parameter-dependence of the splitting probability $\pi_k^{(r)}$ and conditional MFPT $T_k^{(r)}$, which are given by equations (4.17) and (4.24), respectively. We fix the units of time and length by setting the capture rate $\kappa=1$ and the target size $l=1$. (In the case of cytoneme-based transport, for example, a target cell is of size 10 μm so that an array of 10 cells has total length $L=100$ μm. Experimental studies of cytoneme-mediated transport of Wnt morphogens zebrafish

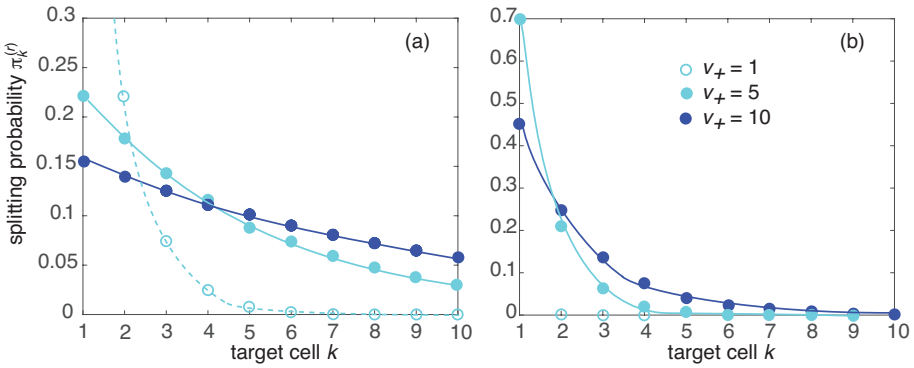

Figure 6: Plot of splitting probability $\pi_k^{(r)}$ as a function of target site k, $k = 1, \ldots, 10$, for various speeds v_+. (a) $r = 0.1$ and (b) $r = 5$.

[33] and Shh in chicken [32] indicate that the growth rate of a cytoneme is of the order $v_+ \sim 0.01 - 0.1$ μm/s and contacts are made every 10^2 seconds, that is, $\kappa \sim 10^{-2}$/s.)

In Fig. 6 we plot $\pi_k^{(r)}$ as a function of k for an array of $N = 10$ targets and various speeds v_+. A number of observations can be made. First, the splitting probability is a monotonically decreasing function of k. As one might expect, targets closer to the origin are more likely to capture the particle. Second, increasing v_+ tends to mitigate this effect, leading to a more even distribution of splitting probabilities. In particular, there is a crossover of the plots for different speeds. In Fig. 7 we show analogous plots for the conditional MFPT $T_k^{(r)}$ in the case of model A. In contrast to the splitting probability, the MFPT depends on the refractory rate η and the retrograde speed v_-. Neither of these parameters qualitatively affects the dependence of $T_k^{(r)}$ on other parameters; decreasing η or v_- simply shifts parameter curves upwards, since it takes more time to escape from the refractory state or return to the origin. For the sake of illustration we set $\eta = v_- = 1$. One would expect the conditional MFPT to increase for more distal targets, and this is confirmed in Fig. 7. It can be seen that $T_k^{(r)}$ grows

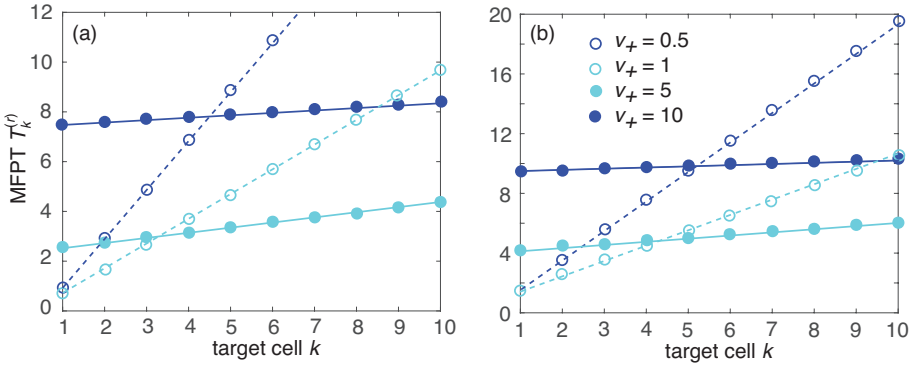

Figure 7: Plot of conditional MFPT $T_k^{(r)}$ as a function of target site k, $k = 1, \ldots, 10$, for various search speeds v_+ (model A). (a) $r = 0.1$ and (b) $r = 1$. Other parameters are $v_- = 1$ and $\eta = 1$.

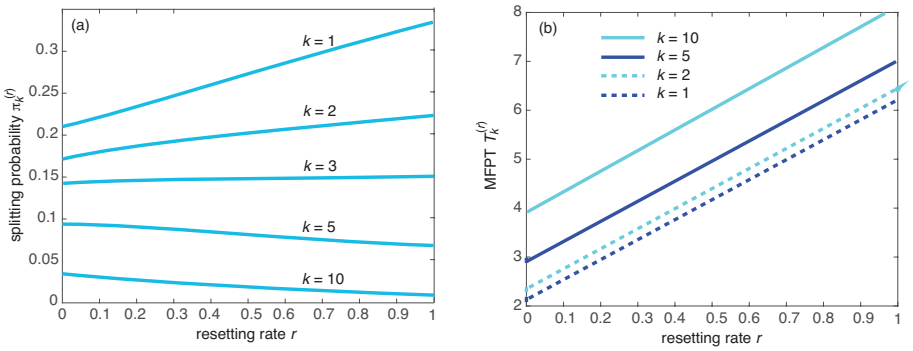

Figure 8: (a) Plot of splitting probability $\pi_k^{(r)}$ as a function of the resetting rate r for various targets k. (a) Corresponding plots of conditional MFPT $T_k^{(r)}$ for model A. Other parameters are $v_+ = 5$, $v_- = 1$ and $\eta = 1$.

approximately linearly with k. Moreover, as with the splitting probability, increasing v_+ tends to flatten the curves so that the MFPT is a weaker function of k and there is a crossover of plots for different speeds.

Fig. 8, we show plots of $\pi_k^{(r)}$ and $T_k^{(r)}$ (model A) as a function of r for various k and fixed speed $v_+ = 5$. It can be seen that the splitting probability increases (decreases) with r in the case of proximal (distal) targets, whereas increasing the resetting rate r leads to an approximately linear increase of $T_k^{(r)}$, irrespective of the target location. (Analogous results were found in [6].) Hence, the inclusion of resetting in model A tends to have a detrimental effect on the conditional MFPTs, since resetting is not required for the particle to return to the origin. On the other hand, the MFPTs are non-monotonic functions of r in the case of model B, as illustrated in Fig. 9(a). This is due to the fact that the MFPTs become infinite in the limit $r \to 0$. There now exists an optimal resetting rate that minimizes $T_k^{(r)}$ for a given k, as was found for

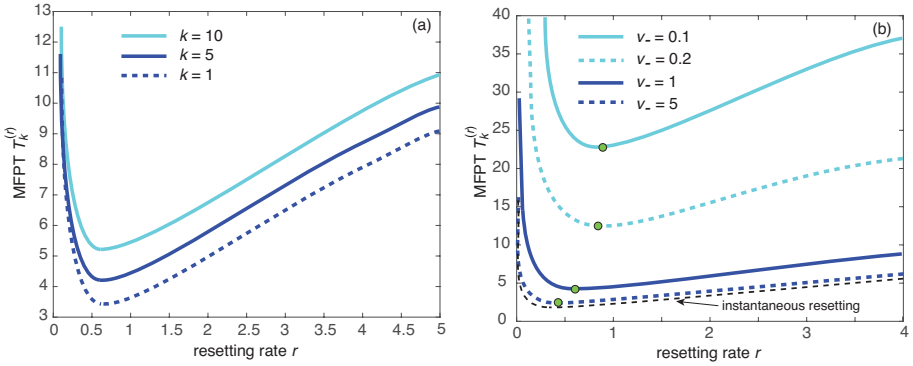

Figure 9: Model B. (a) Plot of conditional MFPT $T_k^{(r)}$ as a function of the resetting rate r for various targets k and $v_- = 1$. (b) Plot of conditional MFPT $T_k^{(r)}$ as a function of the resetting rate r for various return speeds v_- and $k = 5$. Other parameters are $v_+ = 5$ and $\eta = 1$. Green dots indicate optimal resetting rates

a single target in section 3. In Fig. 9(b) we illustrate the effects of a delay on the conditional MFPTs by considering different values of the return speed v_- for a given target cell. As expected, the finite return time increases the conditional MFPT and this effect is larger for slower return speeds v_-. Moreover, decreasing v_- shifts the optimal resetting rate to larger values.

6. Multiple search-and-capture events as a $G/M/\infty$ queue

Now suppose that following absorption by a target, the particle delivers a packet of resources, after which it returns to the origin. It is then supplied with another resource packet and begins a new search-and-capture process. This leads to a sequence of search-and-capture events, whereby resources accumulate in the targets. We also assume that the build up of resources within each target is counterbalanced by degradation, so that there is a steady-state number of packets in the long-time limit. The various stages are illustrated in Fig. 10 for cytoneme-based morphogen transport, where morphogen localized at the tip of a growing cytoneme is delivered as a "morphogen burst" whenever the cytoneme makes temporary contact with a target cell before subsequently retracting. As shown elsewhere [6, 9], for each target the sequence of search-and-capture events can be mapped onto a queuing process as follows: individual resource packets are analogous to customers, the delivery of a packet corresponds to a customer arriving at the service station, and the degradation of a resource packet is the analog of a customer exiting the system after being serviced. Finally, assuming that the packets are degraded independently of each other, the effective number of servers in the corresponding queuing model is infinite, that is, the presence of other customers does not affect the service time of an individual customer. It follows that the relevant queuing model is the $G/M/\infty$ system. Here the symbol G denotes a general customer inter-arrival time distribution $F(t)$, the symbol M stands for a Markovian or exponential service-time distribution $\Phi(t) = 1 - \mathrm{e}^{-\gamma t}$, and '$\infty$' denotes infinite servers. We identify $\phi(t) = -\Phi'(t)$ with the waiting time density for packet degradation at a rate γ.

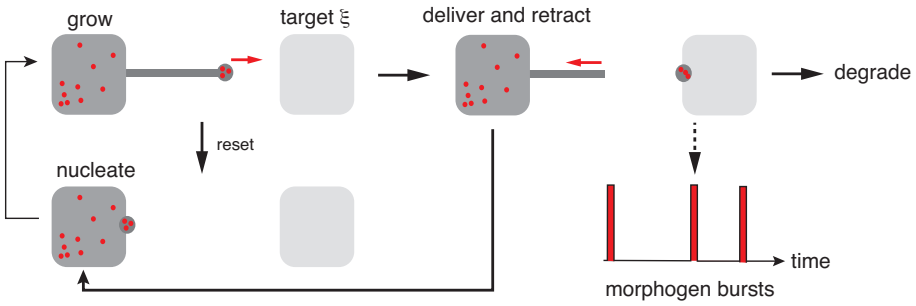

Figure 10: Multiple search-and-capture events for cytoneme-based morphogen transport. Alternating periods of growth, shrinkage, nucleation and target capture generates a sequence of morphogen bursts in a given target cell that is analogous to the arrival of customers in a queuing model. This results in the accumulation of morphogen within the cell, which is the analog of a queue. Degradation corresponds to exiting of customers after being serviced by an infinite number of servers.

It remains to determine the distribution $F(t)$. Recall from section 4 that if a particle starts at $x = 0$ in the search phase, then the splitting probability of being captured by the k-th target is $\pi_k^{(r)}$ and the conditional MFPT for the event is $T_k^{(r)}$, see equations (4.17) and (4.24), respectively. The other $N-1$ targets do not receive any resources. Now suppose that the total time for the particle to deliver its cargo, return to $x = 0$ and start a new search process is given by the random variable $\widehat{\tau}$, which for simplicity is taken to be independent of the location of the target. (This is reasonable if the sum of the mean nucleation time and the mean unloading time is much larger than a typical return time.) Let $n \geq 1$ label the n-th burst event and denote the target that receives the n-th packet by k_n. If T_n is the time of the n-th burst, then

$$T_n = \widehat{\tau}_n + \mathcal{T}_{k_n} + T_{n-1}, \quad n \geq 1, \tag{6.1}$$

with $\mathbb{E}[\mathcal{T}_k] = T_k^{(r)}$. The corresponding inter-arrival times are

$$\Delta_n = \widehat{\tau}_n + \mathcal{T}_{k_n}, \quad n \geq 1.$$

Finally, given an inter-arrival time Δ, we denote the identity of the target that captures the particle by $\mathcal{K}(\Delta)$. We can then write for each target k,

$$\begin{aligned} F_k(t) &= \mathbb{P}[\Delta < t, \mathcal{K}(\Delta) = k] = \mathbb{P}[\Delta < t, |\mathcal{K}(\Delta) = k]\mathbb{P}[\mathcal{K}(\Delta) = k] \\ &= \pi_k^{(r)} \int_0^t \mathcal{F}_k(\Delta) d\Delta, \end{aligned} \tag{6.2}$$

where $\mathcal{F}_k(\Delta)$ is the conditional inter-arrival time density for the k-th target. Let $\rho(\widehat{\tau})$ denote the waiting time density of the delays $\widehat{\tau}_n$. Then

$$\mathcal{F}_k(\Delta) = \int_0^\Delta dt \int_0^\Delta d\widehat{\tau}\delta(\Delta - t - \widehat{\tau}) f_k^{(r)}(t)\rho(\widehat{\tau}) = \int_0^\Delta f_k^{(r)}(t)\psi_1(t-\Delta)dt,$$

where $f_k^{(r)}(t)$ is the conditional first passage time density for a single search-and-capture event that delivers a packet to the k-th target. In particular,

$$T_k^{(r)} = \int_0^\infty t f_k^{(r)}(t) dt. \tag{6.3}$$

Laplace transforming the convolution equation then yields

$$\widetilde{\mathcal{F}}_k(s) = \widetilde{f}_k^{(r)}(s)\widetilde{\rho}(s). \tag{6.4}$$

We now focus on a particular labeled target $k = \xi$. Let $M(t)$ be the number of resource packets in the target that have not yet degraded. In terms of the sequence of arrival times T_n, we can write

$$M(t) = \sum_{n, 0 \leq T_n \leq t} I(t - T_n, S_n)\delta_{k_n,\xi}, \tag{6.5}$$

where

$$I(t - T_n, S_n) = \begin{cases} 1 & \text{if } t - T_n \leq S_n \\ 0 & \text{if } t - T_n > S_n \end{cases}. \tag{6.6}$$

Here S_n is the degradation time of the n-th packet. Introduce the generating function

$$G(z,t) = \sum_{l=0}^\infty z^l \mathbb{P}[M(t) = l], \tag{6.7}$$

and the binomial moments

$$B_m(t) = \sum_{l=r}^{\infty} \frac{l!}{(l-m)!m!} \mathbb{P}[M(t) = l], \quad m = 1, 2, \cdots. \tag{6.8}$$

Suppose that the targets have no resources at time $t = 0$. We will derive an integral equation for the generating function $G(z, t)$. Conditioning the first arrival time by setting $T_1 = y$, we have

$$M(t) = \begin{cases} I(t-y, S_1)\delta_{k_1,\xi} + M^*(t-y) & \text{if } y \le t \\ 0 & \text{if } y > t \end{cases},$$

where $M^*(t)$ has the same distribution as $M(t)$. Note that $I(t-y, S_1)\delta_{k_1,\xi}$ and $M^*(t-y)$ are independent. Moreover,

$$\mathbb{P}[I(t-y, S_1) = j] = [1 - \Phi(t-y)]\delta_{j,1} + \Phi(t-y)\delta_{j,0},$$

so it follows that

$$\sum_{j=0,1} z^j \mathbb{P}[I(t-y, S_1) = j] = z + (1-z)\Phi(t-y).$$

The total expectation theorem then yields

$$\begin{aligned} \mathbb{E}[z^{I(T_1-y,S_1)\delta_{k_1,\xi}}] &= \mathbb{E}\left[\mathbb{E}[z^{I(T_1-y,S_1)}|T_1 = y, k_1 = \xi]\right] \\ &= \int_0^{\infty} [z + (1-z)\Phi(t-y)] dF_\xi(y). \end{aligned}$$

Another application of the total expectation theorem gives

$$\begin{aligned} G(z,t) = \mathbb{E}[z^{M(t)}] &= \mathbb{E}\left[\mathbb{E}[z^{M(t)}|T_1 = y, k_1 = \xi]\right] \\ &= \sum_{k=1}^{N} \int_t^{\infty} dF_k(y) + \int_0^t [z + (1-z)\Phi(t-y)] G(z, t-y) dF_\xi(y) \\ &\quad + \sum_{k \neq \xi} \int_0^t G(z, t-y) dF_k(y). \end{aligned} \tag{6.9}$$

Differentiating equation (6.9) with respect to z and using

$$B_m(t) = \frac{1}{r!} \frac{d^m G(z,t)}{dz^m}\bigg|_{z=1},$$

we obtain an iterative integral equation for the Binomial moments:

$$B_m(t) = \sum_{k=1}^{N} \int_0^t B_m(t-y) dF_k(y) + \int_0^t B_{m-1}(t-y)[1 - \Phi(t-y)] dF_\xi(y). \tag{6.10}$$

In order to obtain the steady-state binomial moments, we Laplace transform equation (6.10) after making the substitutions $dF_k(y) = \pi_k^{(r)} \mathcal{F}_k(y) dy$ and $1 - \Phi(t) = \mathrm{e}^{-\gamma t}$:

$$\widetilde{B}_m(s) = \widetilde{B}_m(s) \sum_{k=1}^{N} \pi_k^{(r)} \widetilde{\mathcal{F}}_k(s) + \pi_\xi^{(r)} \widetilde{\mathcal{F}}_\xi(s) \widetilde{B}_{m-1}(s+\gamma),$$

which can be rearranged to give

$$\widetilde{B}_m(s) = \left[\frac{\pi_\xi^{(r)} \widetilde{\mathcal{F}}_\xi(s)}{1 - \sum_{k=1}^{N} \pi_k^{(r)} \widetilde{\mathcal{F}}_k(s)}\right] \widetilde{B}_{m-1}(s+\gamma). \tag{6.11}$$

Multiplying both sides by s and taking the limit $s \to 0^+$ yields

$$B_m^* := \lim_{t\to\infty} B_m(t) = \lim_{s\to 0^+} s\widetilde{B}_m(s) = \lambda_\xi \widetilde{B}_{m-1}(\gamma),$$

where

$$\lambda_\xi := \lim_{s\to 0^+} \frac{s\pi_\xi^{(r)}\widetilde{\mathcal{F}}_\xi(s)}{1-\sum_{k=1}^N \pi_k^{(r)}\widetilde{\mathcal{F}}_k(s)} = \frac{\pi_\xi^{(r)}}{\sum_{k=1}^N \pi_k^{(r)}(T_k^{(r)}+\langle\widehat{\tau}\rangle)}. \tag{6.12}$$

We have used L'Hopital's rule and equation (6.4), together with the following properties:

$$\widetilde{f}_k^{(r)}(0) = 1 = \widetilde{\rho}(0), \quad \left.\frac{d\widetilde{f}_k^{(r)}}{ds}\right|_{s=0} = -T_k^{(r)}, \quad \left.\frac{d\widetilde{\rho}}{ds}\right|_{s=0} = -\langle\widehat{\tau}\rangle.$$

Equations (6.11) and (6.12) completely determine the steady-state binomial moments. In particular, since $B_0(t) = 1$ and $\widetilde{B}_0(s) = 1/s$, the mean number of packets in the target $k = \xi$ is

$$B_1^* \equiv \langle M\rangle = \lim_{t\to\infty}\langle M(t)\rangle = \frac{\lambda_\xi}{\gamma}. \tag{6.13}$$

Hence, we can interpret λ_ξ as the mean rate at which a packet is delivered to the given target. Similarly,

$$B_2^* \equiv \lim_{t\to\infty}\frac{1}{2}(\langle M(t)^2\rangle - \langle M(t)\rangle) = \lambda_\xi \widetilde{B}_1(\gamma) = \frac{\lambda_\xi}{2\gamma}\frac{\pi_\xi^{(r)}\widetilde{\mathcal{F}}_\xi(\gamma)}{1-\sum_{k=1}^N \pi_k^{(r)}\widetilde{\mathcal{F}}_k(\gamma)}. \tag{6.14}$$

The variance of the number of morphogen packets is

$$\mathrm{Var}[M] = 2B_2^* + B_1^*(1-B_1^*) = \frac{\lambda_\xi}{\gamma}\left[\frac{\pi_\xi^{(r)}\widetilde{\mathcal{F}}_\xi(\gamma)}{1-\sum_{k=1}^N \pi_k^{(r)}\widetilde{\mathcal{F}}_k(\gamma)} + 1 - \frac{\lambda_\xi}{\gamma}\right]. \tag{6.15}$$

Although the mean $\langle M\rangle$ depends on the quantities $\pi_k^{(r)}$ and $T_k^{(r)}$ calculated in section 4 for a single search-and-capture event, the variance depends on the Laplace transform of the full first passage time density $f_k^{(r)}$ according to equation (6.4).

Therefore, suppose that we carry out the leading order asymptotic expansion

$$\widetilde{\mathcal{F}}_k(\gamma) \sim \widetilde{\mathcal{F}}_k(0) + \gamma\left.\frac{d\widetilde{\mathcal{F}}_k}{d\gamma}\right|_{\gamma=0} \approx 1 - \gamma[T_k^{(r)} + \langle\widehat{\tau}\rangle].$$

This will be reasonable provided that $\gamma \ll [T_k^{(r)} + \langle\widehat{\tau}\rangle]^{-1}$ for all k and a chosen range of r. For the parameter values used in Fig. 9(a) we see that $T_k^{(r)} = O(10)$ for $0.1 \le r \le 4$ so the inequality will hold if $\gamma = 0.01$, say. Substituting the approximation into equation (6.15) gives

$$\begin{aligned}\mathrm{Var}[M] &\approx \frac{\lambda_\xi}{\gamma}\left[\frac{1}{\gamma}\frac{\pi_\xi^{(r)}(1-\gamma[T_\xi^{(r)}+\langle\widehat{\tau}\rangle])}{\sum_{k=1}^N \pi_k^{(r)}[T_k^{(r)}+\langle\widehat{\tau}\rangle]} + 1 - \frac{\lambda_\xi}{\gamma}\right]\\ &\approx \langle M\rangle\left\{1-\lambda_\xi(T_\xi^{(r)}+\langle\widehat{\tau}\rangle)\right\}.\end{aligned}$$

At this level of approximation, we see that the Fano factor FF is

$$FF = \frac{\mathrm{Var}[M]}{\langle M\rangle} \approx \left\{1-\lambda_\xi(T_\xi^{(r)}+\langle\widehat{\tau}\rangle)\right\}, \tag{6.16}$$

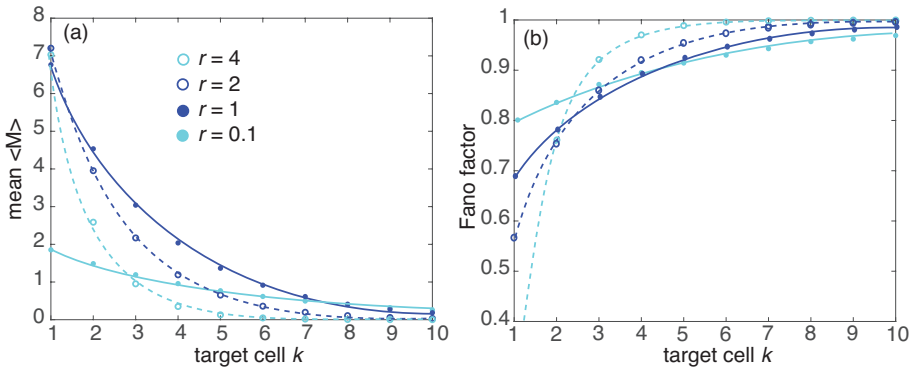

Figure 11: Multiple search-and-capture events for model B. (a) Plots of steady-state mean $\langle M\rangle$ as a function of target label k for various resetting rates. (b) Corresponding plots of the Fano factor. Single-search parameters are $v_+ = 5, v_- = 1, \eta = 1$. Multi-search parameters are $\gamma = 0.01$ and $\langle\widehat{\tau}\rangle = 1$.

which is independent of the degradation rate γ. In Fig. 11 we show sample plots of the mean $\langle M\rangle$ and the Fano factor as a function of target location for various resetting rates r. Corresponding plots as a function of r for various targets k are shown in Fig. 12. The results are based on equations (6.13) and (6.16), respectively. We take the single-search parameters to be the same as Fig. 9(a) for model B, and set $\gamma = 0.01, \langle\widehat{\tau}\rangle = 1$. A number of observations can be made. First, the steady-state mean is a monotonically decreasing function of k. (In the application to cytoneme-based transport this can be interpreted as a morphogen gradient [6].) On the other hand, the Fano factor is an increasing function of k, approaching unity at distal targets. (A Fano factor of one indicates Poisson-like noise.) For a fixed target, the mean is a unimodal function of r whereas the Fano factor is a more complicated function of r and k. The qualitative behavior of the mean and Fano factor as functions of k are

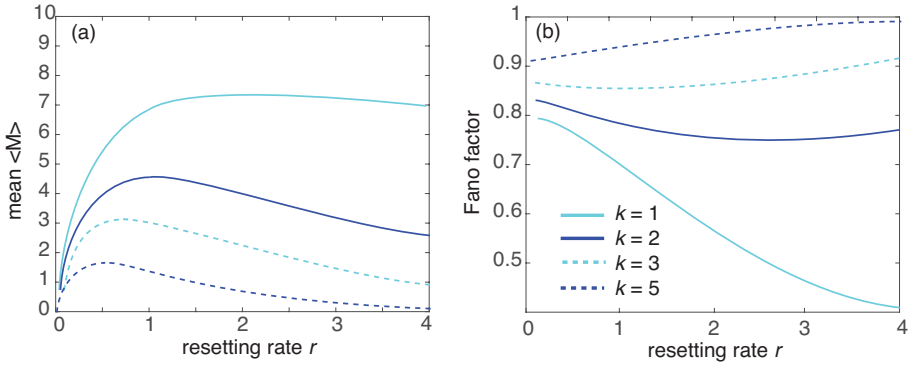

Figure 12: Multiple search-and-capture events for model B. (a) Plots of steady-state mean $\langle M\rangle$ as a function of resetting rate r for various targets. (b) Corresponding plots of the Fano factor. Single-search parameters are $v_+ = 5, v_- = 1, \eta = 1$. Multi-search parameters are $\gamma = 0.01$ and $\langle\widehat{\tau}\rangle = 1$.

similar in model A. However, now $\langle M \rangle$ is a monotonically decreasing function of r, whereas the Fano factor is approximately constant as r is varied.

7. Discussion

In this paper we analyzed a directed search-and-capture model with stochastic resetting, refractory periods and finite return times. We used a probabilistic renewal method to determine the splitting probability $\pi_k^{(r)}$ and MFPT $T_k^{(r)}$ for a particle to be captured by the k-th contiguous target in a 1D array. These are given by equations (4.17) and (4.24), respectively. We also compared search on the bounded domain $[0, L]$ with partially bounded search on the half-line. In the absence of resetting, the probability of target capture was equal to one in the first case but less than one in the second. Hence, the conditional MFPTs for bounded search were monotonically increasing functions of r, whereas the corresponding MFPTs on the half-line were non-monotonic with a minimum at an optimal resetting rate. We also formulated the accumulation of resource packets delivered to the targets by multiple rounds of search-and-capture events as a $G/M/\infty$ queue [9], and used this to calculate the mean and variance of the steady-state number of packets in each target. One obvious extension of the current theory would be to consider search-and-capture processes in higher dimensions. Another would be to consider multiple parallel searchers. One possible complicating factor in the latter case would be molecular crowding and exclusion processes generating correlations between the particles. (See [1] for a recent study of an exclusion process with stochastic resetting.)

One general issue raised by the current study is to what extent there are practical benefits of resetting from the biological perspective. One could argue that in the case of model A, resetting is of little value, since it always leads to a global increase in the MFPT to a target. This reflects the fact that the probability of eventual capture by a target is unity. However, as is clear from Fig. 11, the steepness of the spatial variation of the mean number of resources is sensitive to the value of the resetting rate. In the case of motor-driven transport, it may be desirable to have a more even distribution of resources along an axon [5], which would correspond to the small-r regime. On the other hand, if one were to interpret the resource distribution as a morphogen concentration gradient, then it may be desirable to have a steeper profile, which would correspond to a large-r regime. Model B suggest another possible benefit of resetting, namely, when there is a non-zero probability of failure to find a target, which would result in an infinite MFPT in the absence of resetting. This issue is particularly relevant to higher-dimensional search processes where, for example, a cytoneme may grow in the wrong direction. A similar issue arises in the search-and-capture model of microtubules by kinetochores during cell mitosis [18, 6].

Acknowledgments

PCB was supported by National Science Foundation grant DMS-1613048.

[1] Basu U, Kundu A and Pal A 2019 Symmetric exclusion process under stochastic resetting *Phys. Rev. E* **100** 032136
[2] Belan S 2018 Restart could optimize the probability of success in a Bernouilli trial. *Phys. Rev. Lett.* **120** 080601
[3] Bodrova A S and Sokolov I M 2020 Resetting processes with noninstantaneous return. *Phys. Rev. E* **101** 052130.

[4] Bressloff P C and Newby J M 2013 Stochastic models of intracellular transport. *Rev. Mod. Phys.* **85** 135-196
[5] Bressloff P C and Levien E 2015 Synaptic democracy and active intracellular transport in axons. *Phys. Rev. Lett.* **114** 168101
[6] Bressloff P C and Kim H 2019 Search-and-capture model of cytoneme-mediated morphogen gradient formation *Phys. Rev. E* **99** 052401.
[7] Bressloff P C 2020 Directed intermittent search with stochastic resetting *J. Phys. A: Math. Theor.* **53** 105001
[8] Bressloff P C 2020 Search processes with stochastic resetting and multiple targets *Submitted*
[9] Bressloff P C 2020 Queueing theory of search processes with stochastic resetting *Submitted*
[10] Campos D, Abad E, Mendez V, Yuste S B and Lindenberg K 2015 Optimal search strategies of space-time coupled random walkers with finite lifetimes. *Phys. Rev. E* **91** 052115
[11] Dynes J and Steward O 2007 Dynamics of bidirectional transport of ARC mRNA in neuronal dendrites *J. Comp. Neurol.* **500** 433-447
[12] Evans M R and Majumdar S N 2011 Diffusion with stochastic resetting *Phys. Rev. Lett.***106** 160601
[13] Evans M R and Majumdar S N 2011 Diffusion with optimal resetting *J. Phys. A Math. Theor.* **44** 435001
[14] Evans M R and Majumdar S N 2014 Diffusion with resetting in arbitrary spatial dimension *J. Phys. A: Math. Theor.* **47** 285001
[15] Evans M R and Majumdar S N 2018 Run and tumble particle under resetting: a renewal approach *J. Phys. A: Math. Theor. Math. Theor.* **51** 475003
[16] Evans M R and Majumdar S N 2019 Effects of refractory period on stochastic resetting *J. Phys. A: Math. Theor.* **52** 01LT01
[17] Evans M R, Majumdar S N and Schehr G 2020 Stochastic resetting and applications. *J. Phys. A: Math. Theor.* **53** 193001
[18] Gopalakrishnan M and Govindan B S 2011 A first-passage-time theory for search and capture of chromosomes by microtubules in mitosis. *Bull. Math. Biol.* **73** 2483-2506
[19] Kornberg T B and Roy S 2014 Cytonemes as specialized signaling filopodia. *Development* **141** 729-736
[20] Kusmierz L, Majumdar S N, Sabhapandit S and Schehr G 2014 First order transition for the optimal search time of Levy flights with resetting *Phys. Rev. Lett.* **113** 220602
[21] Maeder C I, San-Miguel A, Wu E Y, Lu H and Shen K 2014 *Traffic* **15** 273-291
[22] Maso-Puigdellosas A, Campos D and Mendez V 2019 Transport properties of random walks under stochastic noninstantaneous resetting. *Phys. Rev. E* **100** 042104
[23] Maso-Puigdellosas A, Campos D and Mendez V 2019 Stochastic movement subject to a reset-and-residence mechanism: transport properties and first arrival statistics. *J. Stat. Mech.* 033201 (2019).
[24] Mulder B M 2012 Microtubules interacting with a boundary: Mean length and mean first-passage times *Phys. Rev. E* **86** 011902
[25] Pal A and Prasad V V 2019 First passage under stochastic resetting in an interval. *Phys. Rev. E* **99** 032123
[26] Pal A, Kusmierz L and Reuveni S 2019 Invariants of motion with stochastic resetting and space-time coupled returns *New J. Phys.* **21** 113024
[27] Pal A, Kusmierz L and Reuveni S 2020 Home-range search provides advantage under high uncertainty. *arXiv:1906.06987* (2020).
[28] Reuveni S, Urbakh M and Klafter J 2014 Role of substrate unbinding in Michaelis-Menten enzymatic reactions *Proc. Natl Acad. Sci. USA* **111** 4391
[29] Rotbart T, Reuveni S and Urbakh M 2015 Michaelis-Menten reaction scheme as a unified approach towards the optimal restart problem *Phys. Rev. E* **92** 060101
[30] Reuveni S 2016 Optimal stochastic restart renders fluctuations in first-passage times universal *Phys. Rev. Lett.* **116** 170601
[31] Rook M S, Lu M and Kosik K S 2000 CamKIIα 3' untranslated regions-directed mRNA translocation in living neurons: Visualization by GFP linkage *J. Neurosci.* **20** 6385-6393
[32] Sanders, T A, Llagostera E and Barna M 2013 Specialized filopodia direct long-range transport of SHH during vertebrate tissue patterning. *Nature* **497** 628-632
[33] Stanganello E and Scholpp S 2016 Role of cytonemes in Wnt transport *J. Cell Sci.* **129** 665-672
[34] Yuste S B, Abad E and Lindenberg K 2013 Exploration and trapping of mortal random walkers. *Phys. Rev. Lett.* **110** 220603